EBioMedicine 28 (2018) 287–302

Contents lists available at ScienceDirect

EBioMedicine

journal homepage: www.ebiomedicine.com

Research Paper

In Vitro Regeneration of Patient-specific Ear-shaped Cartilage and Its First Clinical Application for Auricular Reconstruction

Guangdong Zhou [a,b,d,1], Haiyue Jiang [c,1], Zongqi Yin [a,b,1], Yu Liu [a,b,1], Qingguo Zhang [c], Chen Zhang [e], Bo Pan [c], Jiayu Zhou [c], Xu Zhou [c], Hengyun Sun [c], Dan Li [a,b], Aijuan He [a,b], Zhiyong Zhang [a,b], Wenjie Zhang [a,b], Wei Liu [a,b], Yilin Cao [a,b,c,*]

[a] Shanghai Tissue Engineering Research Key Laboratory, Shanghai Ninth People's Hospital, Shanghai Jiao Tong University School of Medicine, Shanghai, PR China
[b] National Tissue Engineering Center of China, Shanghai, PR China
[c] Auricular Center, Plastic Surgery Hospital, Chinese Academy of Medical Science, Beijing, PR China
[d] Research Institute of Plastic Surgery, Plastic Surgery Hospital, Wei Fang Medical College, Weifang, Shandong Province, PR China
[e] Department of Plastic Surgery, Xin Hua Hospital, Dalian University, Dalian, Liaoning Province, PR China

ARTICLE INFO

Article history:
Received 25 December 2017
Received in revised form 11 January 2018
Accepted 11 January 2018
Available online 13 January 2018

Keywords:
Microtia chondrocytes
Human ear-shaped cartilage
In vitro engineering
3D printing
Polycaprolactone (PCL)
Clinical trial

ABSTRACT

Microtia is a congenital external ear malformation that can seriously influence the psychological and physiological well-being of affected children. The successful regeneration of human ear-shaped cartilage using a tissue engineering approach in a nude mouse represents a promising approach for auricular reconstruction. However, owing to technical issues in cell source, shape control, mechanical strength, biosafety, and long-term stability of the regenerated cartilage, human tissue engineered ear-shaped cartilage is yet to be applied clinically. Using expanded microtia chondrocytes, compound biodegradable scaffold, and *in vitro* culture technique, we engineered patient-specific ear-shaped cartilage *in vitro*. Moreover, the cartilage was used for auricle reconstruction of five microtia patients and achieved satisfactory aesthetical outcome with mature cartilage formation during 2.5 years follow-up in the first conducted case. Different surgical procedures were also employed to find the optimal approach for handling tissue engineered grafts. In conclusion, the results represent a significant breakthrough in clinical translation of tissue engineered human ear-shaped cartilage given the established *in vitro* engineering technique and suitable surgical procedure.
This study was registered in Chinese Clinical Trial Registry (ChiCTR-ICN-14005469).

1. Introduction

Microtia is a congenital malformation of the external ear, with a varied regional prevalence rate of 0.83 to 17.4 per 10,000 births worldwide, and higher prevalence rates in Hispanics and Asians (Bly et al., 2016; Luquetti et al., 2011; Paput et al., 2012). The auricle is an important identifying feature of human face, and hence its deformity has a profound effect on self-confidence and psychological development in the afflicted children. Current cosmetic procedures of treating microtia mainly include the wear of auricular prosthesis, implantation of non-absorbable auricular frame materials or an autologous rib cartilage framework (Bly et al., 2016; Jessop et al., 2016; Wiggenhauser et al., 2017). Non-absorbable frames, such as silastic or high-density polyethylene (Medpor®), generate an excellent ear shape without donor site morbidity, but they lack bioactivity and can lead to extrusion and infections. Autologous rib cartilage transplantation is the current gold-stand treatment for microtia, but harvesting rib cartilage inevitably leads to donor site injury, and replicating the complex 3D ear structure is hard to achieve using surgeons' hand skill, which is highly

Abbreviations: MC, microtia chondrocyte; PCL, polycaprolactone; ChiCTR, Chinese clinical trial registry; ICTRP, International Clinical Trial Registry Platform; SOP, standard operating procedures; PGA, polyglycolic acid; PLA, polylactic acid; GMP, good manufacturing procedure; PBS, phosphate buffered saline; DMEM, Dulbecco's modified Eagle's medium; bFGF, basic fibroblast growth factor; FBS, fetal bovine serum; CAD, computer aided design; CAM, computer aided manufacturing; SEM, scanning electron microscopy; ECM, extracellular matrices; TGF-β1, transforming growth factor-beta1; IGF-I, insulin-like growth factor-I; MRI, magnetic resonance imaging; HE, hematoxylin and eosin; SO/FG, Safranin-O/Fast Green; EvG, Verhoeff van Gieson; HRP, horseradish peroxidase; DAB, diaminobenzidine tetrahydrochloride; Mn, number-average molecular weight; Mw, weight-average molecular weight; SEC, size exclusion chromatography; GAG, glycosaminoglycan.

* Corresponding author at: Shanghai Tissue Engineering Research Key Laboratory, Shanghai Ninth People's Hospital, Shanghai Jiao Tong University School of Medicine; 639 Zhi Zao Ju Road, Shanghai 200011, PR China.
E-mail address: yilincao@yahoo.com (Y. Cao).
[1] These authors are equal to this work.

https://doi.org/10.1016/j.ebiom.2018.01.011

Table 1
Inclusion and exclusion criteria.

- Inclusion criteria
  - ➢ Patient with microtia whose first diagnosis conforms to ICD-10:Q17.20
  - ➢ Patient with grade II or III microtia (cartilage exists in the microtic ear);
  - ➢ Age between 6 and 50 years (when the anesthesia procedures are safe and the ear stops growing);
  - ➢ Healthy, without history of systemic disease.
- Exclusion criteria
  - ➢ Poor state of health;
  - ➢ Local hormone therapy within 3 months;
  - ➢ Blood disease or bleeding tendency;
  - ➢ Drug addiction (including drugs, anesthetic, and alcohol addiction);
  - ➢ Allergic cicatricle physical or physical persons;
  - ➢ Evidence of infection with HIV or hepatitis B or C;
  - ➢ Fever, colds or other symptoms of infection in the current month;
  - ➢ Woman in pregnancy or lactation, or plans to get pregnant within 1 year after initial registration;
  - ➢ Psychological disorder, cannot coordinate with treatment;
  - ➢ Poor development of craniofacial facial nerve;
  - ➢ Major organ malfunction.

depended on the training background and clinical experiences (Breugem et al., 2011; Han et al., 2015; Magritz and Siegert, 2014; Murabit et al., 2010).

Emerging tissue engineering technologies and their successful clinical translation in bone, cartilage, skin, blood vessels, and bladder, provide a novel direction for the treatment of patients with microtia (Atala et al., 2006; Fulco et al., 2014; Makris et al., 2015; Muhart et al., 1997; Olausson et al., 2012). In 1997, the generation of engineered cartilage with human auricular shape in a nude mouse model was reported, which vividly revealed the great potential of tissue engineering for clinical translation (Cao et al., 1997). Since this achievement, many follow-up studies have been published, and cartilage with human ear-shape has been engineered *in vitro*, in nude mice, and in immunocompetent animals using various cells and scaffolds (Bichara et al., 2014; Liu et al., 2010; Reiffel et al., 2013; Shieh et al., 2004; Sterodimas and de Faria, 2013; Zhang et al., 2014; Zheng et al., 2014). However, the clinical application of these technologies remains unreported due to a number of technical issues that need to be addressed, including the lack of proper cell source, the difficulty to generate ear-shaped cartilage with pre-designed 3D structure, the insufficient mechanical properties for shape maintenance, and the unfavorable host response to the engineered graft after its transplantation *in vivo*, etc. (Haisch, 2010; Jessop et al., 2016; Nayyer et al., 2012). To date, the only successful clinical reports of auricular reconstruction with regenerated cartilage have utilized a two-step scaffold-free approach, in which MCs were injected subcutaneously into the lower abdomen, and the regenerated cartilage was further hand-carved into an ear-shaped framework and re-implanted into the final position (Yanaga et al., 2009, 2013). Therefore, the feasibility remains unknown for direct generation of human ear-shaped cartilage *in vitro* and its clinical translation to treat microtia, which would neither depend on surgeons' hand skill nor require the process of heterotopic growth and transplantation.

Recent developments in material science, biofabrication, 3D-printing, and *in vitro* tissue engineering techniques make it possible to design and fabricate a human ear-shaped cartilage *in vitro* for its clinical application. In this study, CT scanning and 3D-printing were employed to direct the fabrication of a biodegradable scaffold which replicated the exact auricular 3D structure symmetrical to the patient's healthy ear and possessed good mechanical properties. After the autologous chondrocytes derived from microtia cartilage (MCs) were seeded onto the scaffold and *in vitro* cultured for 3 months, cartilage frameworks with patient-specific ear-shape were generated and then implanted to reconstruct auricles in five patients with the longest follow-up time of 2.5 years. This paper reports a pilot clinical trial of *in vitro* engineered human ear-shaped cartilage for human auricular reconstruction.

2. Materials and Methods

2.1. Patient Information and Study Design

This study was approved by the Ethical Committee of Plastic Surgery Hospital, Chinese Academy of Medical Sciences, and was registered in Chinese Clinical Trial Registry (ChiCTR), one of primary registers of the WHO International Clinical Trial Registry Platform (ICTRP, http://www.who.int/ictrp/network/chictr2/en/). The registration number for this study is ChiCTR-ICN-14005469). Seed cell expansion and manufacturing of the scaffold were conducted according to the defined standard operating procedures (SOP) and established quality management system approved by National Institutes for Food and Drug Control (identification number: SH201300928 for microtia chondrocytes, and QH201300641 for the scaffold). The manufacturing facilities were approved by Shanghai Food and Drug Packaging Material Control Center (identification number: 20130281).

Five patients (male or female, between 6 and 10 years old) with unilateral microtia were recruited. Table 1 lists the full inclusion and exclusion criteria. Three surgical methods for implanting engineered ear cartilages were respectively adopted according to each patient's physical condition. Table 2 lists the indications and detailed procedures of these three surgical methods. The patients will be followed up intermittently up to 5 years. The primary outcome parameters are the shape, size, and cranio-auricular angle of the reconstructed auricle, which are expected to match those of the contralateral ear. The secondary outcome parameters are the quality of cartilage formation and mechanical property of the reconstructed auricle. The purpose and detailed procedures of this study were explained to the patients and their parents, to whom written informed consent was provided. The current study provides detailed description of a reprehensive case (case 1), a 6-year-old female child, who was the first to receive the tissue engineered ear graft treatment and was followed up for 2.5 years. Preliminary data on the other four on-going cases were also included, and full reporting will be expected after follow up data are completely collected.

A flow chart of the manufacturing and surgical procedure of the first conducted case is shown in Fig. 1. Briefly, CT scanning and 3D reconstruction were applied to obtain a digital image of the patient's healthy contralateral ear (Fig. 1A). A digital mirror-image was created to guide patient's ear reconstruction (Fig. 1B), and a corresponding resin model was generated through 3D-printing (Fig. 1C). This resin ear model was used to cast a pair of negative molds (Fig. 1D), in which biodegradable materials made from polyglycolic acid (PGA, Mw = ~30,000, provided by National Tissue Engineering Center of China, Shanghai, China), polylactic acid (PLA, Mn = ~10,000, Sigma-Aldrich, St. Louis, Mississippi, USA), and polycaprolactone (PCL, Mn = ~60,000, Purac Biochem, the Netherlands) were processed into the ear scaffold with the same shape as the resin positive model (Fig. 1E). At the first stage of surgery, microtia cartilage was harvested for chondrocyte isolation (Fig. 1F1) and a tissue expander was implanted for skin expansion (Fig. 1F2). Patients with low skin tension in the retro-auricular region (such as case 4, which is rare for Asian children) may not require skin expansion. During the period of skin expansion, the isolated microtia chondrocytes (MCs) were expanded (Fig. 1G) and seeded onto the ear scaffold for *in vitro* cartilage engineering (Fig. 1H). After 12 weeks, when a sufficiently-sized skin flap was achieved via tissue expansion and the ear-shaped cartilage was also generated *in vitro*, the second stage surgery was conducted to implant the engineered ear cartilage into the expanded skin flap for auricular reconstruction (Fig. 1I). Post-

Table 2
Three methods applied for auricular reconstruction using the tissue engineered ear graft

Method 1
- Indication: High skin tension in the retroauricular region (common in Asian people); Severe hemifacial microsomia
  - Skin expansion: Yes;
  - Split skin graft transplantation: Yes;
  - Adopted by: case 1, 2, and 5;
  - Surgical procedures:

First stage: Microtia cartilage harvest and tissue expander insertion and inflation
① A 2.0-cm incision was created at the postauricular region;
② The Microtia cartilage was harvested through the incision, and a 80 mL kidney-shaped expander was inserted subcutaneously;
③ The expander was infused intermittently with 0.9% saline solution commencing at the 8th day postoperatively and continued every other day until the volume reached approximately 140 mL and the surface area of the expanded flap reached 9×6 cm^2;
④ Static expansion was kept until the end of total tissue expansion duration (3 months).
Second stage: Auricular reconstruction with tissue engineered ear framework
① Removal of the skin expander: The expander was removed through the same incision created in the first stage surgery. The thickened, edge part of the expander capsule was dissected to loosen the flap. The capsule of the pedicle side was usually reserved.
② The expanded skin flap and a random retroauricular neurovascular fascia flap were prepared;
③ A C-shaped fascia flap was dissected from the retroauricular region superficial to the periosteum;
④ The engineered ear framework was inserted between the fascial flap and the expanded skin flap;
⑤ The fascial flap was sutured to the external ear helix;
⑥ The expanded skin flap was draped over the anterior aspect in a tension-free way and then covered tautly to the framework by means of vacuum drainage
⑦ A split-thickness skin graft was harvested from the groin region and sutured onto the mastoid region to cover the posterior auricular fascial flap.
3rd stage surgery: Modifications of the reconstructed ear
Tragus construction, scar revision, and so on as required.
(Refer to Jiang et al., 2008 for detailed descriptions)

Method 2
- Indication: High skin tension in the retroauricular region (common in Asian people); Unwilling to leave scar by skin harvest
  - Skin expansion: Yes;
  - Split skin graft transplantation: No;
  - Adopted by: Case 3;
  - Surgical procedures:

First stage: Microtia cartilage harvest and tissue expander insertion and inflation
① A 3–4 cm incision was created at the mastoid region;
② The microtia cartilage was harvested and a 80 mL kidney-shaped expander was inserted between the subfascial layer of the non-hair bearing area and the subcutaneous layer of the scalp;
③ The expander was infused intermittently with 4–7 mL 0.9% saline solution commencing at the 7th day postoperatively and continued every other day until the volume reached approximately 140 mL;
④ Static expansion was kept until the end of total tissue expansion duration (3 months).
Second stage: Auricular reconstruction with tissue engineered ear framework
① Removal of the skin expander: Same as method 1
② Insertion of the ear framework beneath the expanded fascial skin flap: An additional horizontal incision was created across the previous incision. The engineered ear framework was inserted into the envelope through the crossing incisions. The expanded flap covered the entire framework.
③ Vacuum drainage: Two negative-pressure drainage tubes were placed in the reconstructed ear, one beneath the anterior side of the flap, the other beneath the posterior side. The outline of the reconstructed ear was clear immediately after suction was applied.
④ Incision closure: The detached scalp of the mastoid region and the incisions were closed using Z-plasty with two-layer suturing. The suction system was removed 7 days after surgery.
Third stage: Modifications of the reconstructed ear
Tragus, earlobe construction, scar revision, and so on as required

Method 3 (the Nagata approach)
- Indication: Low skin tension in the retroauricular region
  - Skin expansion: No;
  - Split skin graft transplantation: Yes;
  - Adopted by: Case 4;
  - Surgical procedures:

First stage: Microtia cartilage harvest
A 2.0-cm incision was created at the mastoid region, through which the microtia cartilage was harvested, and the incision was closed by suture.
Second stage: Auricular reconstruction with tissue engineered ear framework
① Lobule transposition: An anterior and a posterior skin flap from the lobule were created. The posterior flap remains attached to the mastoid skin flap and the anteriorly based tragal flap was used to surface the tragus. A "lazy W-flap" was created by the margins of the mastoid and posterior lobule flap and the middle limbs of the "W" would eventually meet helping form the intertragal notch. This "W-flap" and the anterior lobule flap became transposed in a reciprocal manner resembling a Z-plasty. Vascularity of the W flap was increased by maintaining a subcutaneous pedicle in the floor of the conchal bowl. The above described incisions provided access for creation of the subcutaneous pocket.
② Insertion of the ear framework: The engineered ear framework was introduced into the subcutaneous pocket, a suction drain was positioned beneath the framework, and the flaps were secured over this framework with bolsters. Drains were removed in 48–72 h, and bolsters were removed in 2 weeks.
③ A C-shaped graft engineered using the same approach as the engineered ear framework was "banked" in the subcutaneous layer of the right side abdomen for use in the third stage.
Third stage: Elevation of the reconstructed ear
① Six months after the second stage, the ear framework was elevated from the mastoid skin by dissection into the postauricular sulcus. The postauricular skin was then undermined and advanced into the area of the postauricular sulcus allowing adequate projection of the ear.
② The previously banked C-shaped graft was retrieved, which was then placed under the neoauricle (between the framework and mastoid), and secured by suture. The graft was then covered with a well vascularized tissue to allow for overlying skin graft adherence and prevention of infection or extrusion. A temporoparietal fascia flap was raised and advanced forward to cover the posterior aspect of the neoauricle and the C-shaped graft.
③ A split thickness skin graft was harvested from the groin area to cover the remaining exposed temporoparietal fascia flap. A bolster was then secured into the sulcus with suture. The bolster was kept in place for 1 week.
(Refer to Nagata, 1993 and Shokri and White, 2017 for detailed descriptions)

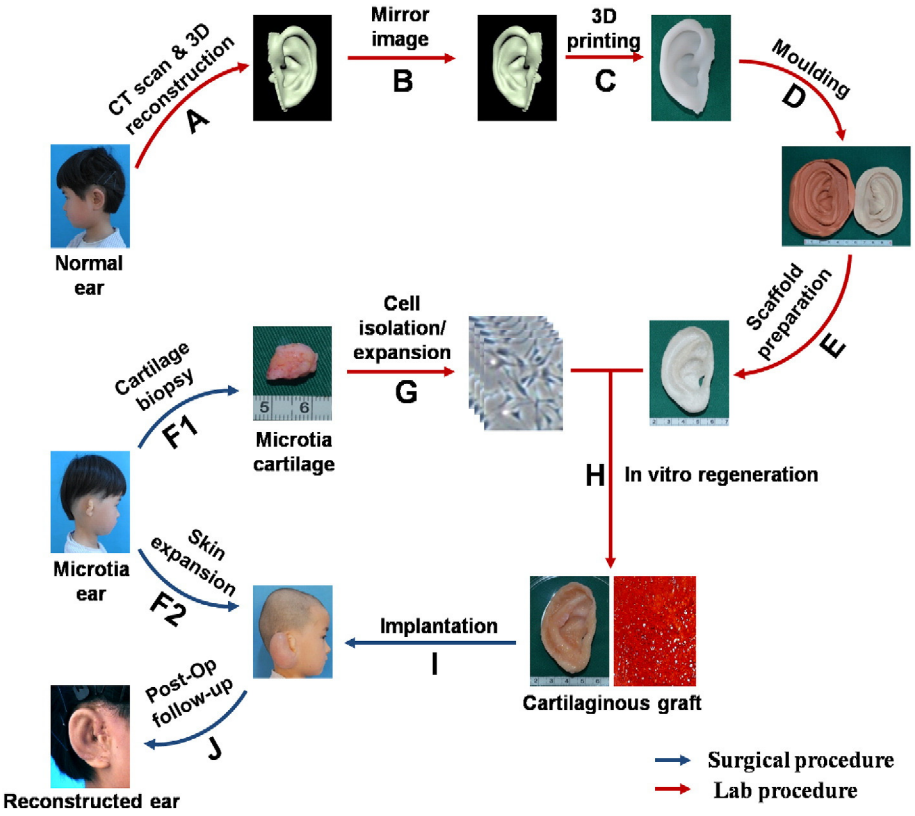

Fig. 1. A flow chart for schematic illustration of auricular reconstruction based on *in vitro* tissue engineered human ear-shaped cartilage.

implantation follow-up assessments were conducted at different time intervals to evaluate the clinical outcomes (Fig. 1J).

2.2. Harvest of Microtia Cartilage and Skin Flap Expansion

For the first conducted case (case 1), a 2.0-cm incision was made at the postauricular region, into which a kidney-shaped expander was inserted subcutaneously. Meanwhile, microtia cartilage (approximately 1.5×1.5 cm^2) was harvested and delivered to the lab which is of good manufacturing procedure (GMP) level for human chondrocyte isolation. The expander was intermittently infused with 0.9% saline solution commencing at the 8th day postoperatively. The infusion was continued every other day until the volume reached approximately 140 mL and the surface area of the expanded flap reached 9×6 cm^2. The skin flap was then kept in a state of static expansion until the end of total tissue expansion duration (3 months). Reviewers may refer to Jiang et al., 2008 for more detailed description. Procedures for the other two methods are listed in Table 2.

2.3. Isolation and Expansion of MCs

The harvested microtia cartilage was carefully dissected to remove fibrous tissue and perichondrium, then fragmented into 1 mm^3 pieces, washed in phosphate buffered saline (PBS) solution containing 100 U/mL penicillin and 100 μg/mL streptomycin, and digested with 0.3% collagenase NB4 (Worthington Biochemical Corp., Freehold, New Jersey, USA) for 8 h at 37 °C. The isolated cells were cultured and expanded in Dulbecco's modified Eagle's medium (DMEM, Gibco BRL, Grand Island, New York, USA) containing 5.0 ng/mL basic fibroblast growth factor (bFGF, R&D Systems Inc., Minneapolis, USA) and 10% fetal bovine serum (FBS, Hyclone, Logan, Utah, USA). Cells in passage 2 were used for *in vitro* cartilage engineering.

2.4. Manufacture of Ear-shaped Scaffold

The ear mold was created according to a previously-described method (Liu et al., 2010). Briefly, the healthy ear of the patient was scanned by CT and the image reflected across the vertical access (with mirror symmetry) by a computer aided design (CAD) system (3DPRO Technology Co., Ltd, Shanghai, China). These data were used to generate the resin ear model via 3D-printing by a computer aided manufacturing (CAM) system (Spectrum 510, Z Corporation, Massachusetts, USA). This 3D-printed ear model was cast by clay and silicone to produce a set of negative molds in which biomaterial scaffolds could be molded into the ear shape identical to the 3D-printed resin ear.

The ear scaffold used a PCL mesh as an inner core, which was wrapped with PGA unwoven fibers and coated with PLA. To generate the inner core, a 9×9 cm^2 PCL mesh with 3×3 mm^2 grids (~1.37 mm in thickness) was 3D-printed. The mesh was pre-shaped by hot (55 °C) compression molding in the negative ear molds and the resulting scaffold was trimmed to make an ear outline. To generate the outer PGA/PLA layers, two pieces (500 mg each) of unwoven PGA fibers were pressed into 8 $\times$ 9 cm^2 sponges respectively, which were then compression-molded by the negative ear molds to generate the ear contour. The PCL inner core was then sandwiched between the pair of PGA layers. The entire scaffold of PCL inner core surrounded by PGA nonwoven fibers was merged by immersion into 0.3% PLA (Sigma Aldrich, Product No. 765112) solution in dichloromethane and hot (55 °C) compression molding again till dry, which was able to partially merge the PGA nonwoven fibers with the PCL core material. The edge of the resultant scaffold was trimmed according to the previous 3D-printed resin ear.

2.5. Biocompatibility Evaluation of the Scaffolds

The cross section of a scaffold piece (1×1 cm^2 with a thickness of 1.5 mm) prepared using the same methods as the ear scaffold was

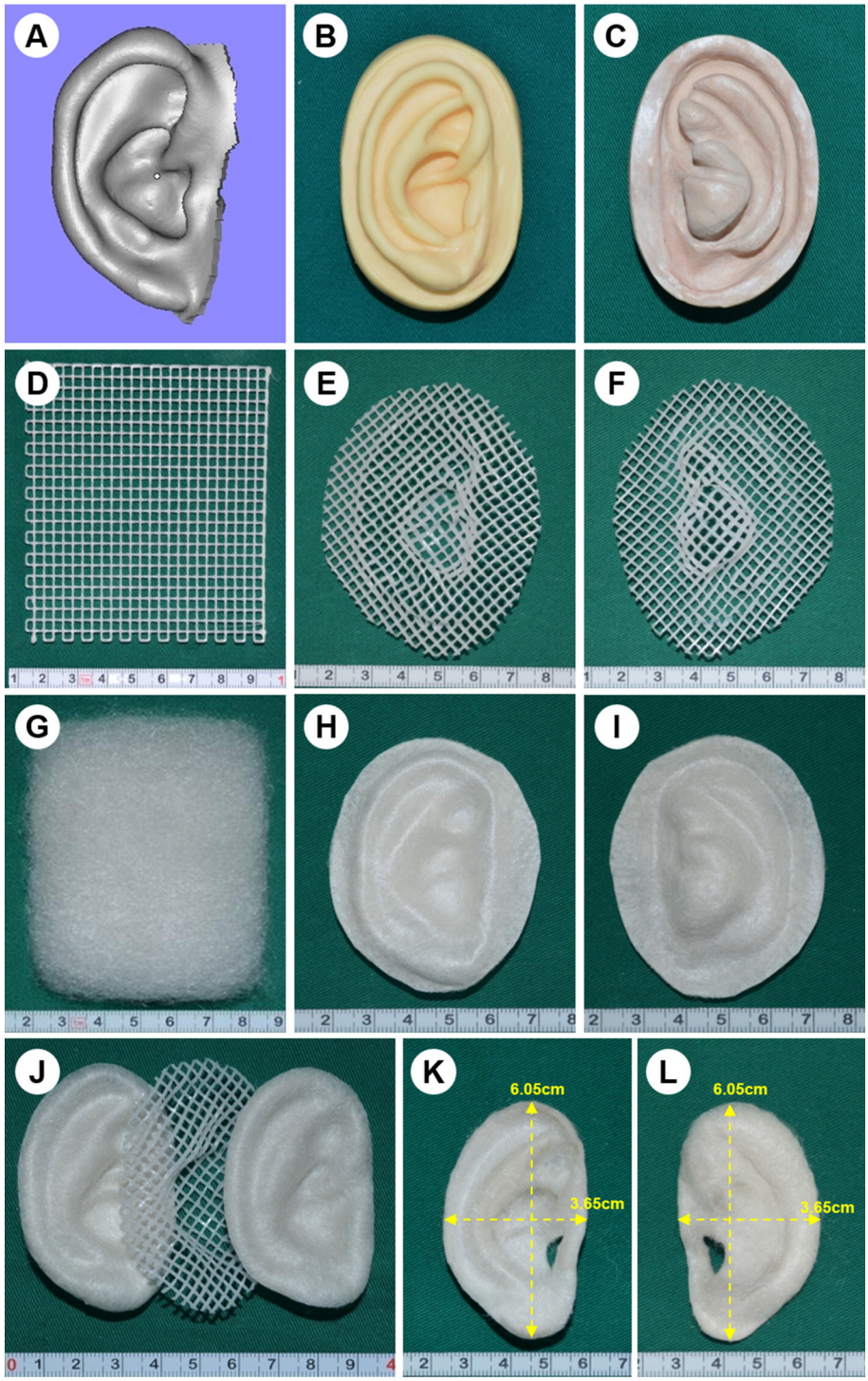

Fig. 2. Preparation of the patient-specific ear-shaped scaffold. The CT reconstructed 3D mirror image of the patient healthy ear is used as a shape model (A), according to which, a pair of negative molds is produced (B, C). PCL mesh is 3D-printed (D) and pre-shaped by the negative molds to generate an ear contour (E, F). Nonwoven PGA fibers are prepared as a sponge (G) and pre-shaped to a pair of ear contours (H, I). The pre-shaped PCL inner core is sandwiched between the pair of pre-shaped PGA layers (J). The whole set of scaffold is coated with PLA, pressed into the ear shape, and trimmed according to the shape of the 3D-printed ear (K, L).

examined by scanning electron microscopy (SEM) (Philips XL-30, Amsterdam, Netherlands) to confirm integration of the PGA fibers with the PCL core. After cell seeding, the chondrocyte-scaffold constructs were also examined by SEM at different culture time points to observe cell attachment and extracellular matrices (ECM) production on the scaffolds.

2.6. In Vitro Engineering of Ear-shaped Cartilage

Expanded MCs (passage 2) at a seeding density of ~4.5×10^8 cells in 5 mL medium (90 million cells/mL) were evenly dropped onto the PGA/PLA layer of the ear-shaped scaffold, followed by 5 h incubation at 37 °C, 5% CO_2. The construct was then cultured in chondrogenic medium

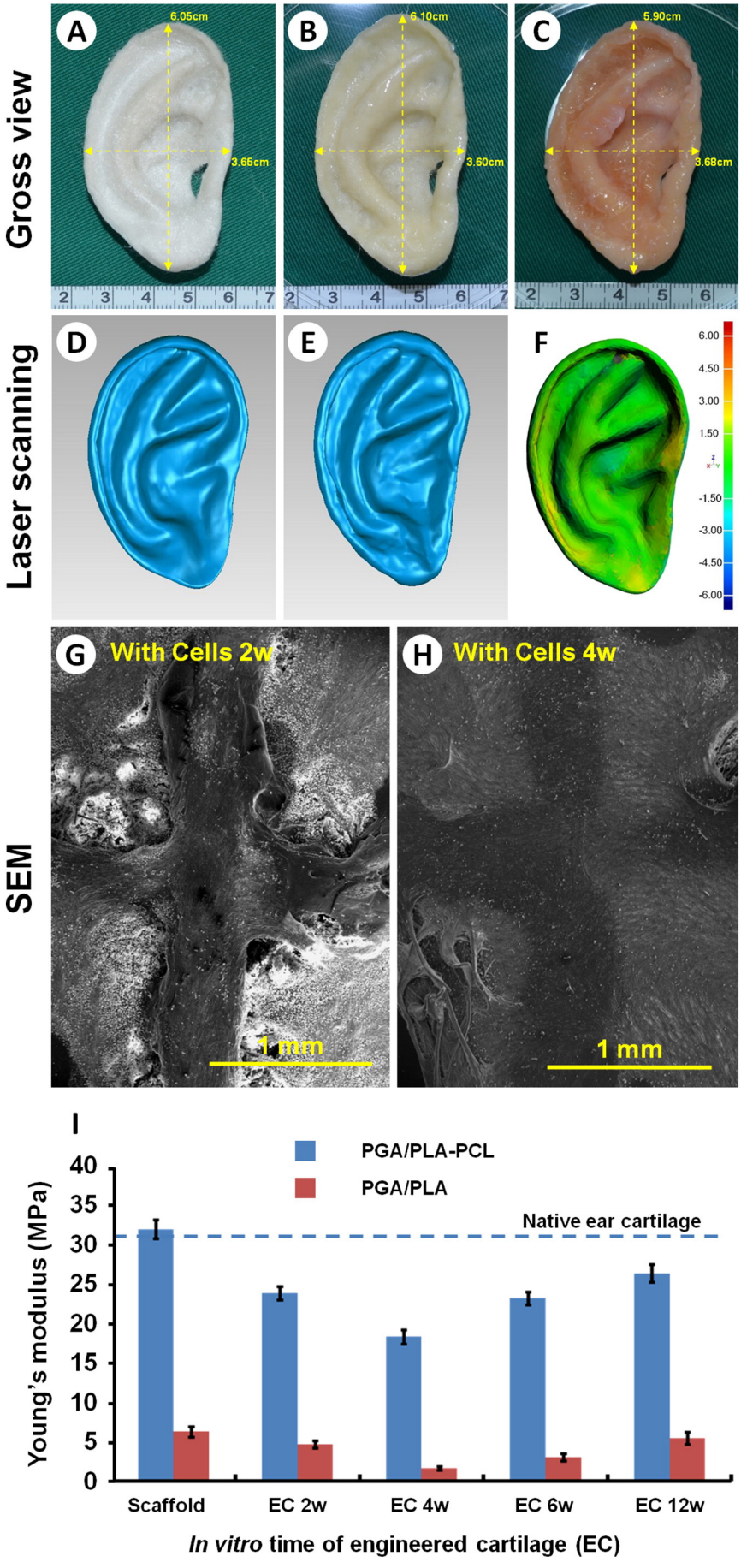
Gross view
A
6.05cm
3.65cm
B
6.10cm
3.60cm
C
5.90cm
3.68cm
Laser scanning
D
E
F
6.00
4.50
3.00
1.50
-1.50
-3.00
-4.50
-6.00
SEM
G With Cells 2w
1 mm
H With Cells 4w
1 mm
I
PGA/PLA-PCL
PGA/PLA
Native ear cartilage
Young's modulus (MPa)
0
5
10
15
20
25
30
35
40
Scaffold
EC 2w
EC 4w
EC 6w
EC 12w
In vitro time of engineered cartilage (EC)

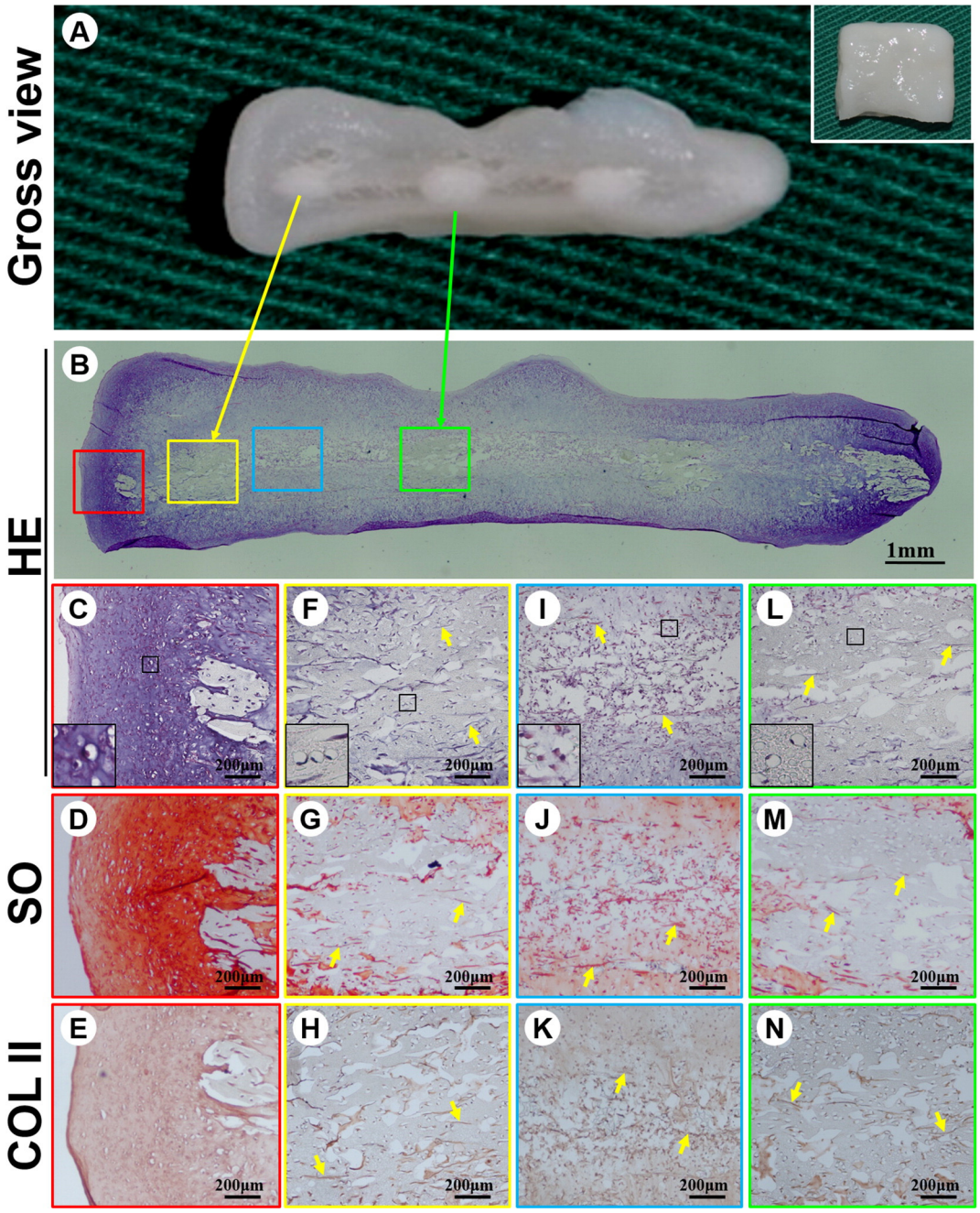

Fig. 4. Cross section and its histological characterization of the in vitro tissue engineered cartilage. The cross section of the engineered cartilage showing a chimeric structure with outer semi-translucent cartilage-like tissue, inner non-transparent PCL grids, and incompact tissue between the PCL bars (A). The outer cartilaginous regions (red frames) showing abundant lacuna structures (B, C) with strong positive SO (D) and collagen II (E) staining. The inner PCL regions (yellow and green frames) corresponding to PCL grid bars contain evenly distributed chondrocytes (B, F–H, L–N). The areas between the grid bars (blue frames) reveal incompact tissue with weak positive SO and collagen II staining (B, I–K). Yellow arrows indicate residual PGA fibers. Black windows indicate the magnified area.

composed of DMEM, 10 ng/mL transforming growth factor beta-1 (TGF-β1, R&D Systems Inc. Minneapolis, USA), 50 ng/mL insulin-like growth factor-I (IGF-I, R&D Systems Inc.), and other supplements (without any serum, all the ingredients of the medium were definable). The medium was changed every other day. The *in vitro* engineered cartilage framework was harvested at the 12th weeks for external ear reconstruction. Before implantation, a cartilage piece (1×1 cm^2 with a thickness of 1.5 mm) engineered with the same method as the ear graft and cultured

Fig. 3. In vitro generation and evaluation of human ear-shaped cartilage. The prepared scaffold shows clear ear features including the helix, anti-helix, triangular fossa, and cavum conchae (A). On cell seeding, the scaffold quickly absorbs the cell suspension (B). After 12 weeks of in vitro culture, the cell-scaffold construct forms a neo-cartilage tissue with the original shape (C). Laser scanning confirms that the shape of the regenerated ear cartilage reaches more than 90% similarity compared with the original scaffold (D–F). SEM confirms good cell compatibility of both the PGA/PLA fibers and PCL core, and ECM coverage of the whole scaffold at week 4 of in vitro culture (G–H). Mechanical testing confirms that the PCL core significantly enhances the mechanical strength of both the scaffold and in vitro engineered cartilage (I). (The laser scanning data were collected from another patient (Case 4): corresponding gross samples are shown in Fig. 9).

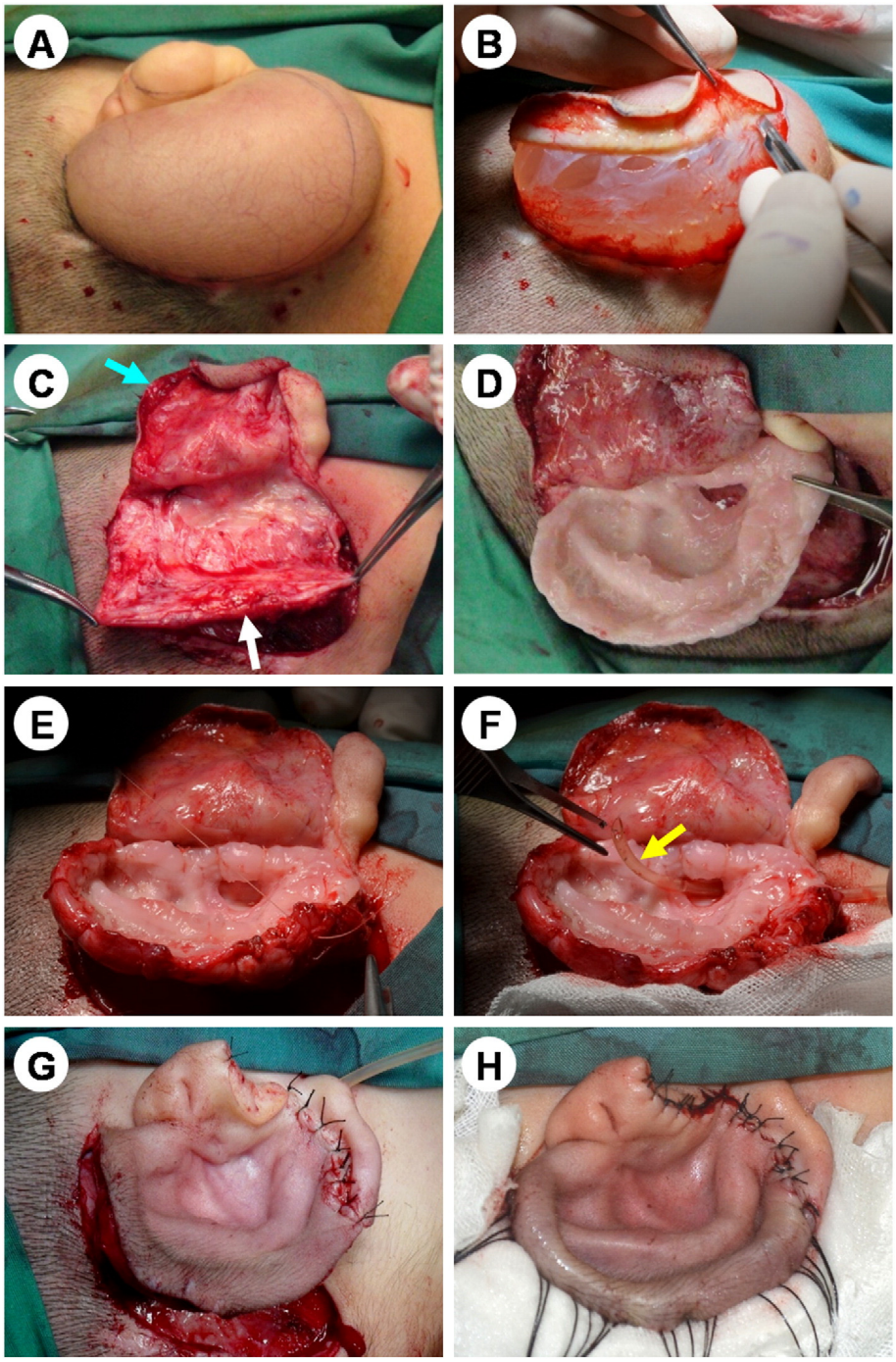

Fig. 5. Surgical implantation procedure of the engineered ear framework. After 12 weeks of skin expansion, a thin kidney-shaped skin capsule with abundant capillaries forms (A). After removing the expander (B), an expanded skin flap (blue arrow) and a post-auricular neurovascular fascia flap (white arrow) are prepared, respectively (C). The in vitro engineered ear framework is inserted between the fascial flap and the expanded skin flap (D). The fascial flap is sutured to the ear framework (E). A small suction drain (yellow arrow) is placed through the ear framework (F). The expanded skin is coapted to the anterior aspect of the framework (G). A skin graft is sutured onto retroauricular and mastoid regions (H).

in the same condition was used for histological and immunohistochemical examinations as a quality control sample. When the control sample was confirmed for obvious cartilage formation and free of contamination, the corresponding ear graft was then released for clinical use.

2.7. Shape Analysis of In Vitro Engineered Human Ear-shaped Cartilage

Surface image data were collected from both the ear-shaped scaffold (before cell seeding) and the ear-shaped cartilage framework (before *in vivo* implantation) by a 3D laser scanning system, in accordance with previously established methods (Liu et al., 2010). The 3D data of the ear framework were compared to those of the ear scaffold with an accepted variation in voxels smaller than 1.5 mm for evaluating the shape similarity level between the ear framework and original scaffold (Liu et al., 2010).

2.8. Implantation of Ear Cartilage Framework

The surgical techniques required for implantation of the engineered ear framework were identical to those established for the autologous rib

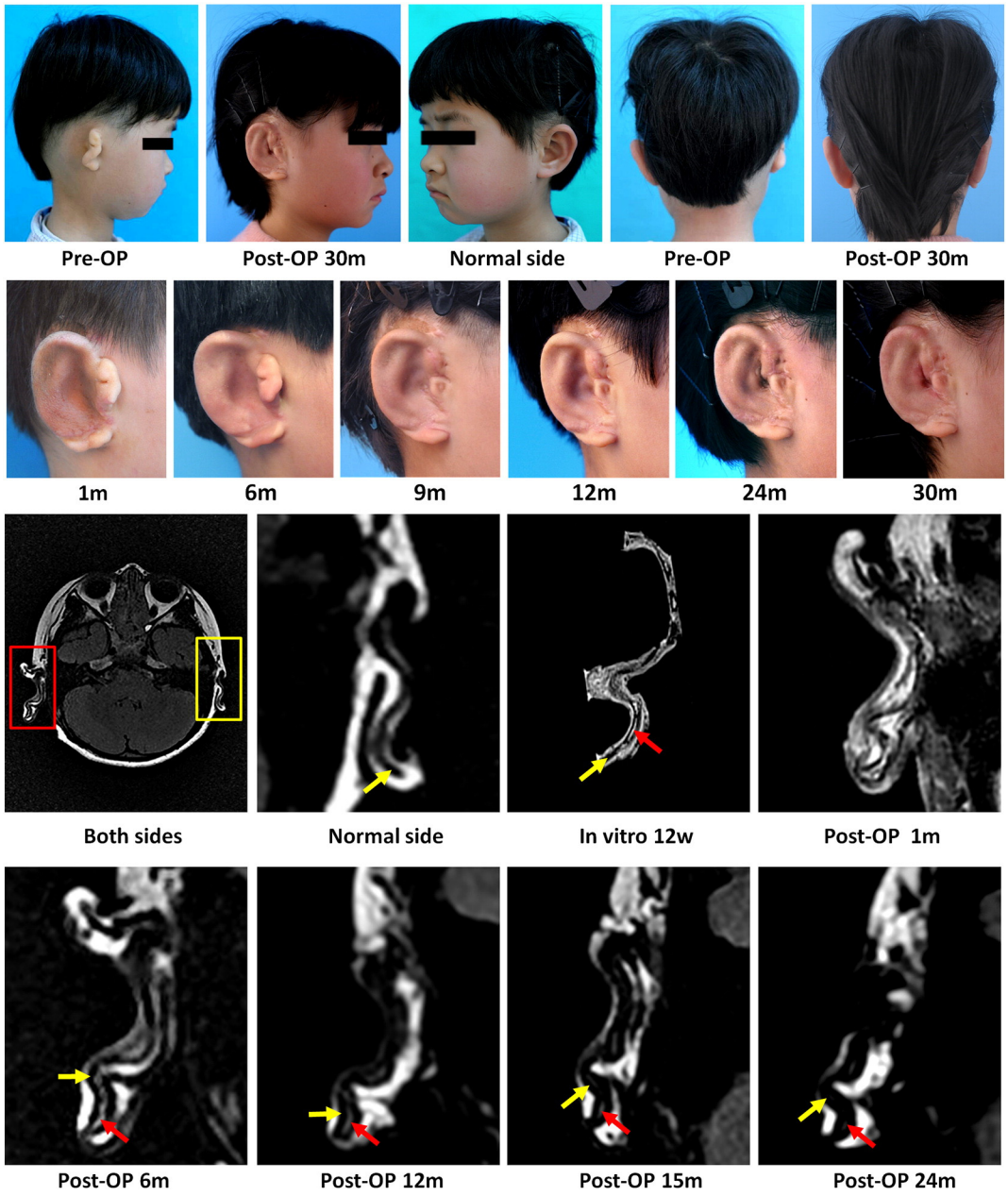

Fig. 6. Post-implantation follow-ups. The pre-operated microtic ear showing a peanut-like structure. At two and a half years post-implantation, the reconstructed ear shows typical auricular features with helix, anti-helix, and cavum conchae, largely symmetrical to the healthy side. Post-implantation assessment at different time points shows the signs of gradual shape recovery, where only blunt ear structures are observed at the 1st and the 6th months post-implantation. Relatively clear ear features with helix, anti-helix, and cavum conchae structures gradually appeared at 9, 12, 24, and 30 months post-implantation. MRI examination reveals an obvious sandwich structure of the ear framework with cartilage (low signal, yellow arrows) surrounding the PCL core region (red arrows). PCL core region signals are difficult to distinguish from other tissue signals at early stage (Post-OP 1 m; a result of tissue edema) and present a gradual decreased trend with increased implantation time (Post-OP 6–24 m). Pre-OP: pre-operation; Post-OP: post-operation.

cartilage framework. For case 1 (Method 1), after removing the skin expander, the skin flap and a random retroauricular neurovascular fascia flap (about 7.0 × 4.5 cm^2) were prepared. During the procedure, care must be taken to avoid vascular compromise of the expanded flap, and a C-shaped fascia flap was dissected from the retroauricular region superficial to the periosteum. The *in vitro* engineered ear framework was then inserted between the fascial flap and the expanded skin flap. The fascial flap was sutured to the external ear helix to cover the posterior aspect of the ear framework. The expanded skin flap was draped over the anterior aspect in a tension-free way and then covered tautly to the framework by means of vacuum drainage. Finally, a split-thickness skin graft, which was harvested from the groin region, was sutured onto the mastoid region to cover the posterior auricular fascial flap. Long sutures were tied over a bolster to tamponade the graft to the recipient bed. A head dressing was applied to protect the engineered ear and all the incisions. Sutures were removed at day 10 post-operation. The main surgical procedures for case 1 were demonstrated in Supplemental Video 1. The above method (method 1) was also applied on cases 2 and 5. Method 2 for case 3 and method 3 for case 4 are listed in Table 2.

2.9. Post-Implantation Follow-Up Assessments

After suture removal, the reconstructed auricle was photographed at 1, 2, 3, 6, 9, 12, 18, 24, and 30 months post-surgery to record swelling, inflammation signs, and shape recovery. Subsequent surgeries were

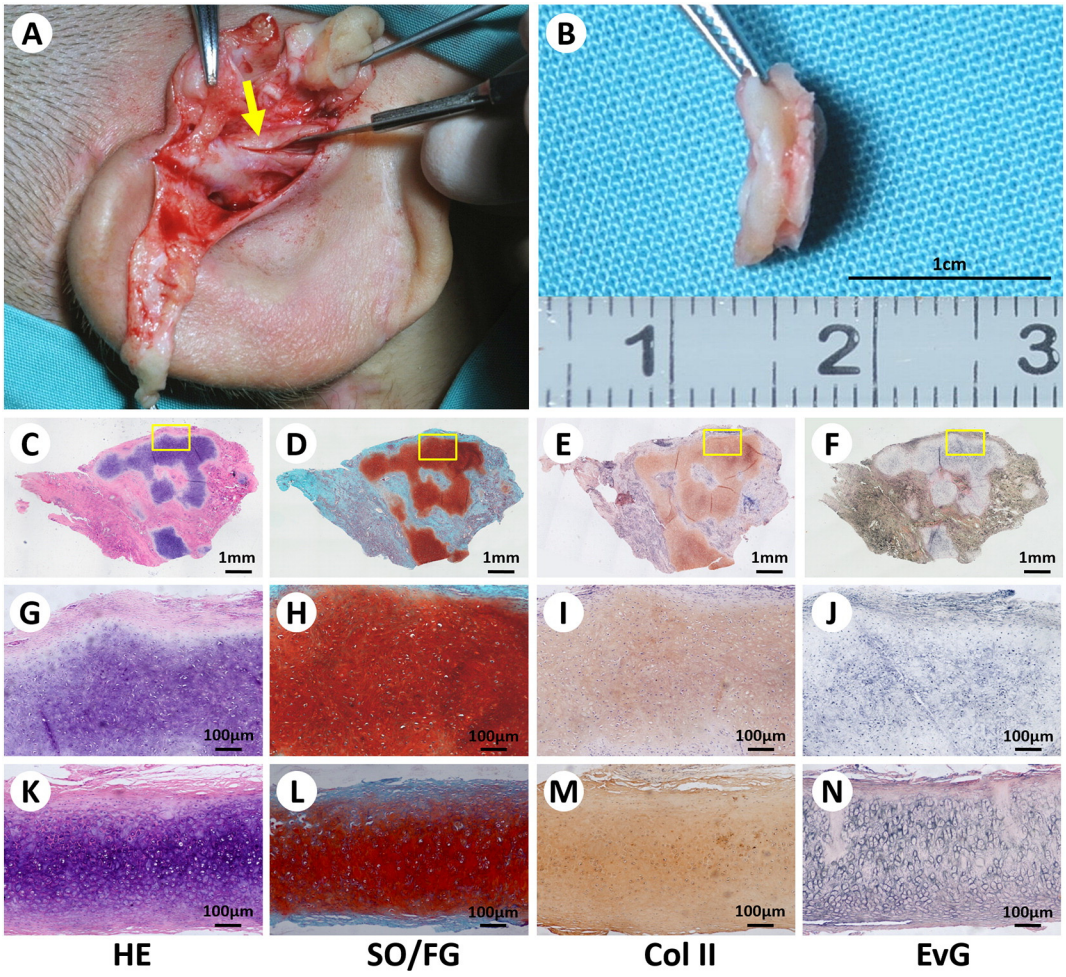

Fig. 7. Gross view and histological characterization of tissue biopsy from the engineered ear at 6 months post-implantation. Biopsy taken from the tragus region of the ear framework (A, yellow arrow). Biopsy showing an ivory-white cartilaginous appearance (B). Histological examination showing typical mature cartilage formation with abundant lacuna structures (C, G) and positive staining of SO/FG (D, H), collagen II (E, I), and EvG (specific staining for elastin) (F, J), similar to native ear cartilage (K–N).

conducted for removing the pedicle of skin flap at 6 months and repairing scar at 18 months, which allowed for tissue biopsies of the implanted ear framework. Both biopsied samples were subjected to histological and immunohistochemical examination to evaluate the state of cartilage formation *in vivo*. Magnetic resonance imaging (MRI) was performed using a 1.5 T MR System at different time points post-implantation to trace the state of cartilage regeneration and PCL core degradation in the implanted ear framework.

2.10. Histological and Immunohistochemical Analysis

Samples from the *in vitro* engineered cartilage piece and *in vivo* biopsied tissue were frozen in liquid nitrogen for cryosection or fixed in 4% paraformaldehyde for 24 h prior to embedding in paraffin. The samples were sectioned into 5-μm slices, mounted on glass slides, and stained with hematoxylin and eosin (HE) or Safranin-O/Fast Green (SO/FG) using previously established protocols (Zhang and Spector, 2009). Detection of elastin was performed using a modified Verhoeff van Gieson (EvG) elastic stain kit (Sigma-Aldrich, St. Louis, Mississippi, USA) following the manufacturer's instructions.

Expression of type II collagen was detected using mouse anti-human type II collagen monoclonal antibody (1:200 in PBS, Santa Cruz, California, USA), followed by incubation of horseradish peroxidase (HRP)-conjugated anti-mouse antibody (1:200 in PBS, Santa Cruz), and color development with diaminobenzidine tetrahydrochloride (DAB, Santa Cruz) (Yan et al., 2009).

2.11. Molecular Weight Assay of PCL

Analyses of number-average molecular weight (Mn) and weight-average molecular weight (Mw) of PCL were conducted by size exclusion chromatography (SEC) at different stages, including raw PCL, PCL core (after 3D-printing and hot compression molding), pre-implantation (after *in vitro* culture for 3 month), and post-implantation (after *in vivo* implantation for 18 months, the sample under evaluation was part of the biopsy taken from case 1 after *in vivo* implantation for 18 months). The PCL degradation profile was revealed according to changes in Mn, Mw, and Mw/Mn (polydispersity) values at different stages.

2.12. Statistical Analysis

All results are expressed as mean ± s.d. Differences among/between experimental groups were analyzed using one-way ANOVA/Student *t*-test. A value of $p < 0.05$ was considered as statistically significant.

3. Results

3.1. Preparation of the Ear Scaffold

The ear scaffold was produced by the processes depicted in Fig. 2. Using these methods, the ear scaffold had a sandwiched structure and

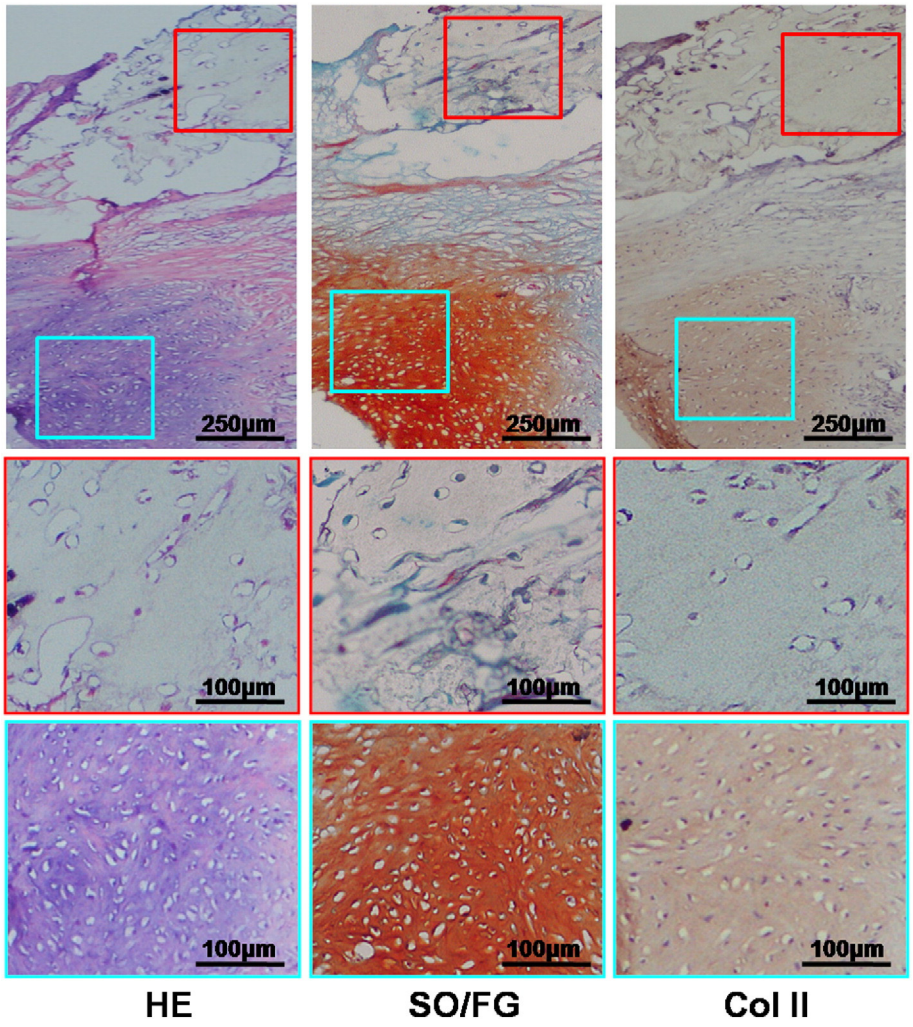

Fig. 8. Histological characterization of the engineered ear biopsy at 1.5 years post-implantation. The biopsy was taken from the cavum conchae region of the ear framework. Histological examination shows a chimeric structure with both cell-infiltrated PCL regions (red frames) and cartilage tissue regions (blue frames), characterized by abundant lacuna structures and positive staining of Safranin-O and collagen II.

presented the mirror image of the patient's normal ear with detailed structures including the helix, anti-helix, triangular fossa, and cavum conchae (Fig. 2K, L). The cross-section of a scaffold piece, produced using the same method as the ear scaffold, presented a chimeric structure with outer PGA fibers and inner PCL grid bars (Supplemental Fig. 1A). It is worth noting that the PCL bars themselves also showed a chimeric structure, where PGA fibers were evenly embedded within the PCL matrix (Supplemental Fig. 1B–F), indicating that the hot compression process was able to partially merge the PGA fibers with the PCL core.

3.2. In Vitro Engineering of Ear-shaped Cartilage Framework

In our cell expansion conditions, MCs underwent robust proliferation (Supplemental Fig. 2) and the expanded cells showed good chondrogenic function after being seeded onto PGA/PLA scaffold and *in vitro* cultured for 12 weeks (Supplemental Fig. 3). Approximately 4.5×10^6 MCs were originally isolated from the microtia cartilage. These cells were expanded to about 4.5×10^8 cells at passage 2. After being seeded onto the ear scaffold, the cell suspension was quickly absorbed and distributed throughout the whole scaffold (Fig. 3A–B, G). After 12 weeks of *in vitro* culture, a cartilage-like framework was formed and the original ear shape was largely retained (Fig. 3C) which was also supported by the histological examination of similarly engineered cartilage peace (Fig. 4). Laser scanning analysis showed that the shape of the regenerated ear at 12 weeks attained >90% similarity compared with the shape of the original scaffold (Fig. 3D–F), indicating that accurate shape control of the *in vitro* engineered cartilage could be achieved by controlling the shape of its scaffold.

Scanning electron microscopy examination revealed that cells were evenly distributed among the PGA fibers and PCL core, and gradually produced ECM to cover the whole scaffold with increased *in vitro* culture time (Fig. 3G, H; Supplemental Fig. 4). No obvious cell detachment was observed during *in vitro* culture, implying good cell affinity to both PGA fibers and PCL core. It is worth noticing that the mechanical strength of the *in vitro* engineered constructs was significantly enhanced by the PCL core and reached a 4-fold increase compared with that of the constructs without the PCL core (Fig. 3I), which contributed to the shape maintenance after *in vivo* implantation.

The cross section of a regenerated cartilage piece engineered in the same way as the ear framework (a quality control sample) showed a chimera structure, in which the outer cartilaginous tissue surrounded and covered the inner PCL grids, with incompact tissue observed between the grid bars (Fig. 4A). Histological examination further confirmed typical cartilage features at the outer layer, with abundant lacuna structures, glycosaminoglycan (GAG) deposition, and collagen II expression (Fig. 4B–E). In the central part, un-degraded PCL regions (corresponding to the PCL bars) and incompact tissue between bars were observed (Fig. 4F–N). It is worth noticing that high numbers of chondrocytes were observed in the PCL bar regions with a pore

Fig. 9. Four other cases of auricular reconstruction based on in vitro engineered ear graft. Four other patients also received engineered ear grafts and were being followed-up. Similar *in vitro* and clinical outcomes corresponding to case 1 was obtained.

structure and containing only a few PGA residues (Fig. 4F–H, L–N). Transformation of the PCL bar regions, from PGA fiber/PCL chimeric structures (Supplemental Fig. 1) to porous chondrocyte/PCL chimeric structures (Fig. 4F–H, L–N), implied that the pore structure of the PCL bars resulted from PGA degradation during *in vitro* culture, thus providing a path for cell infiltration. In the region between the grid bars, consistent with the gross view, incompact tissue with the un-degraded PGA residues was observed (Fig. 4I–K). Importantly, after 3 months of *in vitro* culture, the PGA fibers were mostly degraded with abundant cartilage ECM formation (especially those in the outer layer) (Fig. 4A–E). This occurrence would likely reduce direct exposure of the existing PGA residuals to the immune system, and therefore alleviate the host responses towards the engineered graft, as we have previously demonstrated (Luo et al., 2009; Liu et al., 2017).

3.3. Implantation of the Ear Framework

After 12 weeks of skin expansion, a kidney-shaped skin capsule was formed and abundant capillaries were distinctly observed in the expanded skin (Fig. 5A). After removing the expander and stripping the fibrous capsule, an expanded skin flap and a post-auricular neurovascular fascia flap were prepared (Fig. 5B, C). The *in vitro* engineered ear framework was then inserted between the fascial flap and the expanded skin flap, and fixed by suturing the fascial flap to the helix (Fig. 5D, E). The expanded skin flap was used to cover the frontal surface of the ear framework, which was tightly attached to the flap under negative pressure of the suction drain and comprised detailed structures of auricular helix, anti-helix, triangular fossa, and cavum conchae (Fig. 5F–H). The main surgical procedures were demonstrated in Supplemental Video 1 and the ear framework displayed a cartilage-like appearance with mechanical properties strong enough for surgical handling.

3.4. Post-Implantation Follow-Up of Auricular Outline

Within the first two weeks, the reconstructed ear showed obvious edema with a blurring shape (data not shown). After two weeks, the edema slowly reduced and the shape of the reconstructed ear, as well as the color of the covered skin, gradually recovered (Fig. 6). Within 6 months post-implantation, only the basic ear contour was observed, while key auricular structures, such as helix, triangular fossa, anti-helix, and cavum conchae, became gradually distinct after 9 months (Fig. 6). It was worth noticing that at 12 months, the reconstructed auricle presented high stiffness and low flexibility (Supplemental Video 2), whereas at 24 months, an obvious improvement in flexibility with more distinct structures were achieved (Supplemental Video 3; Fig. 6).

The molecular weight assay of the PCL core revealed a decline trend in both Mn and Mw at different time points, indicating slow degradation of the PCL (Supplemental Fig. 5). These results were further supported by the gradual decline in MRI signals in the PCL core regions with increased post-implantation time. In particular, a significant decrease was observed at 24 months post-implantation (Fig. 6, red arrowed), which provided a reasonable explanation for improved flexibility at 2 years.

Table 3
Summary of the total five cases.

	Age	Gender	Diagnosis (Weerda's classification)	Surgical method for graft implantation	Follow-up period	Outcome
Case 1	6	F	Unilateral grade III microtia, right side.	Method 1	2.5 years	• Obvious cartilage formation before implantation • Shape, size and cranioauricular angle match the contralateral normal ear • Landmark structures are distinct • Obvious post-Op cartilage formation • No sign of absorption or extrusion
Case 2	9	F	Grade III microtia on the right side; grade I microtia on the left side.	Method 1	1.5 years	• Obvious cartilage formation before implantation • Cranioauricular angle match the contralateral ear. • Helix and cavum conchae are distinct, triangular fossa and anti-helix are vague. • No obvious cartilage formation at the biopsy site after 6 m. • No sign of absorption or extrusion
Case 3	8	F	Unilateral grade III microtia, right side	Method 2	1 year	• Obvious cartilage formation before implantation • Shape, size and cranioauricular angle match the contralateral normal ear. • Landmark structures are distinct • Obvious cartilage formation at the biopsy site after 6 m. • Slight distortion occurred after 6 m post surgery
Case 4	7	M	Unilateral grade III microtia, right side	Method 3	6 months	• Obvious cartilage formation before implantation • Shape and size match the contralateral normal ear • Landmark structures are distinct • Obvious cartilage formation after 6 m post implantation • Slight distortion occurred after the second stage surgery (creation of the cranioauricular angle)
Case 5	7	F	Unilateral grade II microtia, right side	Method 1	2 months	• Obvious cartilage formation before implantation • Shape, size and cranioauricular angle match the contralateral normal ear • Landmark structures are distinct • Obvious post-Op cartilage formation • No sign of absorption or extrusion

3.5. Histological Examinations of In Vivo Regenerated Cartilage

During the procedure of skin flap pedicle removal at 6 months post-implantation, a biopsy was taken from the tragus region of the ear framework (Fig. 7A). The biopsied tissue showed an ivory-white cartilaginous appearance (Fig. 7B). Histological examinations revealed typical cartilage formation with abundant lacuna structures, GAG deposition, and strong collagen II expression (Fig. 7C–E, G–I), similar to the native ear cartilage (Fig. 7K–M). Particularly, the expression of elastin (indicated by EvG staining) was also detected in the regenerated cartilage (at a slightly lower level than that in native cartilage) (Fig. 7F, J, N), indicating the formation of elastic cartilage. No PCL core was observed in this sample as a result of the biopsy location. At 18 months post-implantation, further scar revision procedure was performed, which allowed a very small biopsy to be obtained from the cavum conchae region of the ear framework. Histological examinations showed that a chimeric structure with both undegraded PCL (Fig. 8, red frames) and cartilage-like tissue characterized by abundant lacuna structures and positive staining of SO/FG and collagen II (Fig. 8, blue frames). Most importantly, consistent with the histological findings before implantation, scattered cells were still detected in the PCL regions (Fig. 8, red frames), indicating good cell compatibility of the PCL core.

3.6. Post-Implantation Follow-Up of Four Other Cases

Four other cases, in which patients had received an engineered ear transplant and were being followed-up, revealed similar *in vitro* and clinical outcomes corresponding to the first patient (Fig. 9). Among the total five cases, four cases showed obvious cartilage formation after 6 months post implantation. Summary for all five patients is provided in Table 3. Owing to the short follow-up period, full examination data will be provided in future. Note that one original case failed to show up for all of the post-surgery follow-ups after the second stage surgery and therefore was removed from the current trial. An additional case (case 5 in Fig. 9) was thus enrolled instead of the original one to make up five cases in total.

4. Discussion

Tissue engineered auricle is a promising alternative to current ear reconstructive options, but its clinical translation is yet to be accomplished. In the current study, cartilage frameworks with patient-specific ear shapes and proper mechanical strength were successfully engineered *in vitro*. Using these engineered ear frameworks, we performed external ear reconstruction on 5 patients and achieved satisfactory therapeutic outcome as revealed during 2.5 years' follow-up so far. The achievement of this clinical translation should be attributed to the integration and innovation of several strategies, including using expanded MCs as seed cell source, *in vitro* culture to alleviate the host response towards the implanted graft, CAD-CAM for patient-specific cartilage shape control, and PCL inner core for long-term shape maintenance.

Microtia chondrocytes have been proposed as a promising cell source due to their abilities to form elastic cartilage and since they can be isolated from the patient's microtic ear without injuring healthy cartilage (Ishak et al., 2015; Kamil et al., 2004; Kobayashi et al., 2011; Nakao et al., 2017). In the current study, the patient's MCs that were expanded in a condition containing bFGF demonstrated the abilities of robust proliferation, 3D cartilage generation, and stable subcutaneous cartilage formation, which confirmed their candidacy as a practical cell source to engineer auricular cartilage for clinical application.

Polylactic acid (PLA) coated PGA, as the traditional synthetic scaffold employed by many pioneered tissue engineering studies, is especially suitable for engineering cartilage with complex shape due to its controllable mechanical properties and shape processing (Cao et al., 1997; Mooney et al., 1996). However, PGA/PLA could induce significant host response once implanted in immunocompetent mammals, leading to the failure of cartilage formation (Ceonzo et al., 2006; Haisch, 2010; Rotter et al., 2005). In the current study, an *in vitro* engineering strategy

was applied, which allowed sufficient degradation of the PGA/PLA scaffold and abundant deposition of the autologous cartilage ECM and thus greatly reduced direct exposure of PGA fibers to the immune system. This procedure can therefore alleviate the host responses as we previously demonstrated (Luo et al., 2009, 2013; Liu et al., 2017). In addition, *in vitro* culture also allows for quality assessments of the engineered cartilage before transplantation.

Generally, *in vitro* engineered ear cartilage is usually too weak to maintain its complex 3D structures after its implantation under skin tension. In the current study, by means of combining CT scanning, CAD-CAM, and 3D-printing technologies, we were able to generate a PCL inner core supported PGA/PLA scaffold that not only replicated the patient-specific ear structures, but also provided mechanical support for shape maintenance of the patient-specific cartilage regeneration *in vitro* and *in vivo*.

The advantages of using mechanically stiff material as an inner stent to support the ear shape of the engineered cartilage has been described by previous researchers (Bichara et al., 2014). However, most of them used non-degradable materials (such as titanium wire), which is likely to be extruded after a certain time period. The current study used PCL as the inner core, which can be biodegraded by hydrolysis of its ester linkages in a slow manner so that the engineered cartilage may have sufficient time to mature and gain mechanical properties while gradually replacing the degrading inner core (Yan et al., 2009). According to literature, complete degradation of PCL *in vivo* requires 2–4 years (Höglund et al., 2007; Hutmacher et al., 2001; Oh et al., 2011; Sun et al., 2006; Tuba et al., 2014; Woodruff and Hutmacher, 2010). As this particular case has been followed up for 2.5 years and plus 3 months of *in vitro* culture, the PCL frame has already undergone over 2 years' degradation, by which time a significant portion of PCL has degraded as confirmed by MRI examination, whereas the engineered ear cartilage remained able to retain its original 3D shape supported with significantly decreased stiffness and increased elasticity, indicating that it was the regenerated cartilage rather than the PCL core that maintained the ear shape. Meanwhile, we have previously shown that *in vivo* regenerated cartilage itself without PCL frame had mechanical properties similar to those of native cartilage (Yan et al., 2009). In the current study, histological examination of the biopsied samples revealed formation of mature *in vivo* cartilage at 6 m and 18 m post-Op (Figs. 7 and 8). Obviously, the mechanical support contributed by the engineered cartilage should not be denied. Moreover, the low melting point (63 °C) of PCL allowed a small portion of PGA fibers to fuse themselves into the PCL grids during hot compression molding, making the PCL porous for cell infiltration after PGA degradation, which further facilitates the replacement of the inner core with the patient's own tissue during PCL degradation.

The current trial included five patients. The engineered ear graft for each of the total five patients showed excellent cartilage formation *in vitro* with detailed ear structure, indicating that the procedures for engineering the ear graft were feasible and repeatable. We adopted 3 surgical methods to implant the engineered ear grafts to the 5 patients according to each patient's retro-auricular skin condition. Among the 3 methods, method 1 is suitable for most Asian children who have tight retro-auricular skin and thus need skin expansion. Method 1 also used a facial flap to cover the back and the helix rim of the engineered ear graft, which not only provided sufficient blood supply, but also protected the graft from extrusion. Therefore, method 1 was applied on cases 1 (the first conducted case), 2, and 5 and achieved satisfactory shape maintenance and cartilage formation outcomes. Unlike cases 1 and 5, case 2 normal side external ear did not have the distinctive auricular features, which might reflect somewhat level of deformity on the non-microtia side. Although the detailed 3D ear structure was a bit compromised, the outcome of clinical repair largely replicated the other side ear morphology (Fig. 9). In addition, the patient seemed to exhibited pro-fibrotic condition as the expanded skin contracted more severely than other cases, which might also contribute to the structure compromise. Among 5 cases, cartilage was not observed in the biopsied tissue of case 2, which might be caused by non-suitable location of the biopsy or the fibrosis of implanted cartilage. The variation of clinical outcome due to individual conditions such as pro-inflammatory/pro-fibrotic is also commonly observed in conventional ear reconstruction using rib cartilage framework (Davis, 1956).

To avoid skin graft and scar formation on donor site wound, method 2, which used expanded skin only to cover the implanted engineered graft, was tried on the case 3. This method has also been widely applied on Asian children. Because the engineered graft was covered with the expanded skin only without fascial flap, which caused much thinner soft tissue covering and thus rendered the grafts relatively higher risk of extrusion as the engineered ear graft was relatively thinner with relatively sharper edges when compared to the conventional ear framework carved from rib cartilage.

Case 4 had low skin tension in the reto-auricular area, so we adopted method 3 (the Nagata approach) on this patient to avoid the process of skin expansion. This method needed more cartilaginous graft to make the ear framework as well as the C-shaped base to elevate the ear framework in a secondary surgery. Our tissue engineering method can provide sufficient cartilaginous grafts without harming the normal cartilage, but the elevation step could expose the newly implanted ear framework to surgical trauma again shortly after its implantation, which may aggravate the inflammatory reaction caused by the previous surgery and lead to long lasting edema which may compromise the ear shape. Therefore, the selection of an optimal surgical procedure for handling and implanting the engineered ear graft is extremely important. Besides, the *in vitro* engineered ear graft (neocartilage) was more delicate and fragile than the graft carved from the fully developed rib cartilage, and the acute inflammatory trauma environment as well as the excessive handling during surgery may reduce the viability of the resident chondrocytes of the engineered ear graft, thus, hindering the subsequent chondrogenesis and shape maintenance after implantation. Moreover, developing more mature cartilaginous grafts to ease the surgical handling is also important for the widespread application of engineered ear graft in future.

In summary, we were able to successfully design, fabricate, and regenerate patient-specific external ears. The first clinical study of translating the well-known human-ear-shaped cartilage from nude mouse to human may represent a follow-up significant achievement in the field of tissue engineering after its original experimental study (Cao et al., 1997). Nevertheless, further efforts remain necessary to eventually translate this prototype work into routine clinical practices. In the future, long-term (up to 5 years) follow-up of the cartilage properties and clinical outcomes after complete degradation of the PCL inner core will be essential. In addition, further optimization and standardization in scaffold fabrication, cell expansion, *in vitro* cartilage engineering, surgical procedures, as well as multi-center clinical trials would also be the targets for the future investigations. 3D bioprinting (print with cells) for direct fabrication of ear-shaped cartilage may also be a future direction (Kang et al., 2016).

Supplementary data to this article can be found online at https://doi.org/10.1016/j.ebiom.2018.01.011.

Acknowledgments

This research was supported by National Natural Science Foundation of China (81671837, 31271046, 81371703, 81371701, and 81571823), Hi-Tech Research and Development Program of China (2012AA020507), Shanghai Science and Technology Committee (13DZ0503100, 16QB1400600), Capital Clinical Specialty Application Research Program (Z151100004015185), and National Key Clinical Specialist Construction Program of China. The authors appreciate the surgical assistant from the medical and nurse staff at the Auricular Center, Plastic Surgery Hospital, Chinese Academy of Medical Science, Beijing, China; Research Institute of Plastic Surgery, Plastic Surgery Hospital, Wei Fang Medical College, Weifang, Shandong, China; and Department

of Plastic Surgery, Xin Hua Hospital, Dalian University, Dalian, Liaoning, P.R. China. We also appreciate the language editing from Dr. Kara Spiller of Drexel University.

Funding Sources

The sponsors of the study had no roles in study design, data collection, data analysis, data interpretation, or writing of the report. All authors had full access to all data of this study and had final responsibility for the decision to submit for publication.

Conflicts of Interest

We declare that we have no conflicts of interest.

Author Contributions

GZ was the principal investigator of the grant supporting the current scientific work, conceived the overall technical procedures and participated in surgical design with detailed supervision particularly on scaffold design, manufacture, and *in vitro* cartilage engineering; GZ also significantly contributed to the preparation of this report by initial draft, data collection and interpretation, and figure preparation. HJ was responsible for the surgical design and performed main surgery and peri-operative care. ZY performed most of the primary technical work, including scaffold preparation, cell isolation and culture, *in vitro* cartilage reconstruction, exanimations for cartilage formation, and primary data collection. YL was responsible for the technical design, developed the key techniques for shape control, ear scaffold manufacture, massive expansion of microtia chondrocytes, and *in vitro* regeneration of ear-shaped-cartilage based on these cells. YL also significantly contributed to the manuscript drafting, data interpretation, and figure preparation. QZ, CZ, BP, JZ, XZ, and HS participated in the surgical design and were responsible for the post-operative care and data collection from the five patients. DL and AH helped to conduct the primary experiment. ZZ, WZ, and WL participated in overall design and manuscript preparation, and WL advised overall manuscript structure, edited and finalized the report. YC was the principal investigator on the grant supporting the preliminary and current work, proposed, supervised, and participated in the whole project including design of the whole clinical trial, scaffold modification, *in vitro* ear cartilage engineering, clinical procedure and follow-up, and data collection and interpretation.

References

Atala, A., Bauer, S.B., Soker, S., Yoo, J.J., Retik, A.B., 2006. Tissue-engineered autologous bladders for patients needing cystoplasty. Lancet 367, 1241–1246.

Bichara, D.A., Pomerantseva, I., Zhao, X., Zhou, L., Kulig, K.M., Tseng, A., Kimura, A.M., Johnson, M.A., Vacanti, J.P., Randolph, M.A., Sundback, C.A., 2014. Successful creation of tissue-engineered autologous auricular cartilage in an immunocompetent large animal model. Tissue Eng. Part A 20, 303–312.

Bly, R.A., Bhrany, A.D., Murakami, C.S., Sie, K.C., 2016. Microtia reconstruction. Facial Plast. Surg. Clin. North Am. 24, 577–591.

Breugem, C.C., Stewart, K.J., Kon, M., 2011. International trends in the treatment of microtia. J. Craniofac. Surg. 22, 1367–1369.

Cao, Y., Vacanti, J.P., Paige, K.T., Upton, J., Vacanti, C.A., 1997. Transplantation of chondrocytes utilizing a polymer-cell construct to produce tissue-engineered cartilage in the shape of a human ear. Plast. Reconstr. Surg. 100, 297–302.

Ceonzo, K., Gaynor, A., Shaffer, L., Kojima, K., Vacanti, C.A., Stahl, G.L., 2006. Polyglycolic acid-induced inflammation: role of hydrolysis and resulting complement activation. Tissue Eng. 12, 301–308.

Davis, W.B., 1956. Absorption of autogenous cartilage grafts in man. Brit. J. Plast. Surg. 9, 177–185.

Fulco, I., Miot, S., Haug, M.D., Barbero, A., Wixmerten, A., Feliciano, S., Wolf, F., Jundt, G., Marsano, A., Farhadi, J., Heberer, M., Jakob, M., Schaefer, D.J., Martin, I., 2014. Engineered autologous cartilage tissue for nasal reconstruction after tumour resection: an observational first-in-human trial. Lancet 384, 337–346.

Haisch, A., 2010. Ear reconstruction through tissue engineering. Adv. Otorhinolaryngol. 68, 108–119.

Han, S.E., Lim, S.Y., Pyon, J.K., Bang, S.I., Mun, G.H., Oh, K.S., 2015. Aesthetic auricular reconstruction with autologous rib cartilage grafts in adult microtia patients. J. Plast. Reconstr. Aesthet. Surg. 68, 1085–1094.

Höglund, A., Hakkarainen, M., Albertsson, A.C., 2007. Degradation profile of poly(ε-caprolactone)—the influence of macroscopic and macromolecular biomaterial design. J. Macromol. Sci. A 44, 1041–1046.

Hutmacher, D.W., Schantz, T., Zein, I., Ng, K.W., Teoh, S.H., Tan, K.C., 2001. Mechanical properties and cell cultural response of polycaprolactone scaffolds designed and fabricated via fused deposition modeling. J. Biomed. Mater. Res. 55, 203–216.

Ishak, M.F., See, G.B., Hui, C.K., Abdullah, A., Saim, L., Saim, A., Idrus, R., 2015. The formation of human auricular cartilage from microtic tissue: an in vivo study. Int. J. Pediatr. Otorhinolaryngol. 79, 1634–1639.

Jessop, Z.M., Javed, M., Otto, I.A., Combellack, E.J., Morgan, S.N., Breugem, C.C., Archer, C.W., Khan, I.M., Lineaweaver, W.C., Kon, M., Malda, J., Whitaker, I.S., 2016. Combining regenerative medicine strategies to provide durable reconstructive options: auricular cartilage tissue engineering. Stem Cell Res Ther 7 (19).

Jiang, H., Pan, B., Lin, L., Cai, Z., Zhuang, H., 2008. Ten-year experience in microtia reconstruction using tissue expander and autogenous cartilage. Int. J. Pediatr. Otorhinolaryngol. 72, 1251–1259.

Kamil, S.H., Vacanti, M.P., Vacanti, C.A., Eavey, R.D., 2004. Microtia chondrocytes as a donor source for tissue-engineered cartilage. Laryngoscope 114, 2187–2190.

Kang, H.W., Lee, S.J., Ko, I.K., Kengla, C., Yoo, J.J., Atala, A., 2016. A 3D bioprinting system to produce human-scale tissue constructs with structural integrity. Nat. Biotechnol. 34, 312–319.

Kobayashi, S., Takebe, T., Inui, M., Iwai, S., Kan, H., Zheng, Y.W., Maegawa, J., Taniguchi, H., 2011. Reconstruction of human elastic cartilage by a CD44+ CD90+ stem cell in the ear perichondrium. Proc. Natl. Acad. Sci. U. S. A. 108, 14479–14484.

Liu, Y., Zhang, L., Zhou, G., Li, Q., Liu, W., Yu, Z., Luo, X., Jiang, T., Zhang, W., Cao, Y., 2010. In vitro engineering of human ear-shaped cartilage assisted with CAD/CAM technology. Biomaterials 31, 2176–2183.

Liu, Y., Li, D., Yin, Z., Luo, X., Liu, W., Zhang, W., Zhang, Z., Cao, Y., Liu, Y., Zhou, G., 2017. Prolonged in vitro precultivation alleviates post-implantation inflammation and promotes stable subcutaneous cartilage formation in a goat model. Biomed. Mater. 12, 15006.

Luo, X., Zhou, G., Liu, W., Zhang, W.J., Cen, L., Cui, L., Cao, Y., 2009. In vitro precultivation alleviates post-implantation inflammation and enhances development of tissue-engineered tubular cartilage. Biomed. Mater. 4, 25006.

Luo, X., Liu, Y., Zhang, Z., Tao, R., Liu, Y., He, A., Yin, Z., Li, D., Zhang, W., Liu, W., Cao, Y., Zhou, G., 2013. Long-term functional reconstruction of segmental tracheal defect by pedicled tissue-engineered trachea in rabbits. Biomaterials 34, 3336–3344.

Luquetti, D.V., Leoncini, E., Mastroiacovo, P., 2011. Microtia-anotia: a global review of prevalence rates. Birth Defects Res. A. Clin. Mol. Teratol. 91, 813–822.

Magritz, R., Siegert, R., 2014. Auricular reconstruction: surgical innovations, training methods, and an attempt for a look forward. Facial Plast. Surg. 30, 183–193.

Makris, E.A., Gomoll, A.H., Malizos, K.N., Hu, J.C., Athanasiou, K.A., 2015. Repair and tissue engineering techniques for articular cartilage. Nat. Rev. Rheumatol. 11, 21–34.

Mooney, D.J., Mazzoni, C.L., Breuer, C., McNamara, K., Hern, D., Vacanti, J.P., Langer, R., 1996. Stabilized polyglycolic acid fibre-based tubes for tissue engineering. Biomaterials 17, 115–124.

Muhart, M., McFalls, S., Kirsner, R., Kerdel, F., Eaglstein, W.H., 1997. Bioengineered skin. Lancet 350, 1142.

Murabit, A., Anzarut, A., Kasrai, L., Fisher, D., Wilkes, G., 2010. Teaching ear reconstruction using an alloplastic carving model. J. Craniofac. Surg. 21, 1719–1721.

Nagata, S., 1993. A new method of total reconstruction of the auricle for microtia. Plast. Reconstr. Surg. 92, 187–201.

Nakao, H., Jacquet, R.D., Shasti, M., Isogai, N., Murthy, A.S., Landis, W.J., 2017. Long-term comparison between human normal conchal and microtia chondrocytes regenerated by tissue engineering on nanofiber polyglycolic acid scaffolds. Plast. Reconstr. Surg. 139 (911e-21e).

Nayyer, L., Patel, K.H., Esmaeili, A., Rippel, R.A., Birchall, M., O'Toole, G., Butler, P.E., Seifalian, A.M., 2012. Tissue engineering: revolution and challenge in auricular cartilage reconstruction. Plast. Reconstr. Surg. 1123–1137.

Oh, S.H., Park, S.C., Kim, H.K., Koh, Y.J., Lee, J.H., Lee, M.C., Lee, J.H., 2011. Degradation behavior of 3D porous polydioxanone-b-polycaprolactone scaffolds fabricated using the melt-molding particulate-leaching method. J. Biomater. Sci. Polym. Ed. 22, 225–237.

Olausson, M., Patil, P.B., Kuna, V.K., Chougule, P., Hernandez, N., Methe, K., Kullberg-Lindh, C., Borg, H., Ejnell, H., Sumitran-Holgersson, S., 2012. Transplantation of an allogeneic vein bioengineered with autologous stem cells: a proof-of-concept study. Lancet 380, 230–237.

Paput, L., Czeizel, A.E., Banhidy, F., 2012. Possible multifactorial etiology of isolated microtia/anotia—a population-based study. Int. J. Pediatr. Otorhinolaryngol. 76, 374–378.

Reiffel, A.J., Kafka, C., Hernandez, K.A., Popa, S., Perez, J.L., Zhou, S., Pramanik, S., Brown, B.N., Ryu, W.S., Bonassar, L.J., Spector, J.A., 2013. High-fidelity tissue engineering of patient-specific auricles for reconstruction of pediatric microtia and other auricular deformities. PLoS One 8, e56506.

Rotter, N., Ung, F., Roy, A.K., Vacanti, M., Eavey, R.D., Vacanti, C.A., Bonassar, L.J., 2005. Role for interleukin 1alpha in the inhibition of chondrogenesis in autologous implants using polyglycolic acid-polylactic acid scaffolds. Tissue Eng. 11, 192–200.

Shieh, S.J., Terada, S., Vacanti, J.P., 2004. Tissue engineering auricular reconstruction: in vitro and in vivo studies. Biomaterials 25, 1545–1557.

Shokri, T., White, D.R., 2017. The Nagata technique for microtia reconstruction. Oper. Tech. Otolaryngol. Head Neck Surg. https://doi.org/10.1016/j.otot.2017.03.009.

Sterodimas, A., de Faria, J., 2013. Human auricular tissue engineering in an immunocompetent animal model. Aesthet. Surg. J. 33, 283–289.

Sun, H., Mei, L., Song, C., Cui, X., Wang, P., 2006. The in vivo degradation, absorption and excretion of PCL-based implant. Biomaterials 27, 1735–1740.

Tuba, F., Olah, L., Nagy, P., 2014. Towards the understanding of the molecular weight dependence of essential work of fracture in semi-crystalline polymers: a study on poly(ε-caprolactone). Express Polym Lett 8, 869–879.
Wiggenhauser, P.S., Schantz, J.T., Rotter, N., 2017. Cartilage engineering in reconstructive surgery: auricular, nasal and tracheal engineering from a surgical perspective. Regen. Med. 12, 303–314.
Woodruff, M.A., Hutmacher, D.W., 2010. The return of a forgotten polymer—polycaprolactone in the 21st century. Prog. Polym. Sci. 35, 1217–1256.
Yan, D., Zhou, G., Zhou, X., Liu, W., Zhang, W.J., Luo, X., Zhang, L., Jiang, T., Cui, L., Cao, Y., 2009. The impact of low levels of collagen IX and pyridinoline on the mechanical properties of in vitro engineered cartilage. Biomaterials 30, 814–821.
Yanaga, H., Imai, K., Fujimoto, T., Yanaga, K., 2009. Generating ears from cultured autologous auricular chondrocytes by using two-stage implantation in treatment of microtia. Plast. Reconstr. Surg. 124, 817–825.
Yanaga, H., Imai, K., Tanaka, Y., Yanaga, K., 2013. Two-stage transplantation of cell-engineered autologous auricular chondrocytes to regenerate chondrofat composite tissue: clinical application in regenerative surgery. Plast. Reconstr. Surg. 132, 1467–1477.
Zhang, L., Spector, M., 2009. Comparison of three types of chondrocytes in collagen scaffolds for cartilage tissue engineering. Biomed. Mater. 4 (45012).
Zhang, L., He, A., Yin, Z., Yu, Z., Luo, X., Liu, W., Zhang, W., Cao, Y., Liu, Y., Zhou, G., 2014. Regeneration of human-ear-shaped cartilage by co-culturing human microtia chondrocytes with BMSCs. Biomaterials 35, 4878–4887.
Zheng, R., Duan, H., Xue, J., Liu, Y., Feng, B., Zhao, S., Zhu, Y., Liu, Y., He, A., Zhang, W., Liu, W., Cao, Y., Zhou, G., 2014. The influence of Gelatin/PCL ratio and 3-D construct shape of electrospun membranes on cartilage regeneration. Biomaterials 35, 152–164.